Atomic and Subatomic Imaging and Spectroscopy

Mater. Res. Soc. Symp. Proc. Vol. 839 © 2005 Materials Research Society P1.3

Tomographic Imaging of Nanocrystals by Aberration-Corrected Scanning Transmission Electron Microscopy

Klaus van Benthem, Yiping Peng, Stephen J. Pennycook
Oak Ridge National Laboratory, One Bethel Valley Road, Oak Ridge, TN 37831-6031, USA

ABSTRACT

In aberration corrected scanning transmission electron microscopy, the depth of focus is of the order of a few nanometers, so that the three-dimensional shape of nanocrystals could so far not be determined with atomic resolution. Here we show that with the assistance of image simulations it is possible to achieve atomic-scale information in the depth direction by analyzing a through-focal series where the number of atoms in most columns can be determined by Z-contrast simulations. The error in this analysis is about two atoms in the thickest regions, and less in thinner regions.

INTRODUCTION

Three-dimensional microscopy at atomic resolution has been a long-term goal of materials science. Transmission electron microscopy is known to produce two-dimensional projections of real 3D structures. Recently, it became possible to explore three-dimensional nanostructures by applying tilt-series electron tomography [1-3] or atom-probe microscopy [4]. In scanning transmission electron microscopy (STEM), one benefit of aberration correction is that the increased probe aperture angle results in a decreased depth of focus [5]. It thus becomes possible to focus on different depths within a sample, and a through-focal series now becomes a through-depth series which can be recombined into a 3D data set. van Benthem and co-workers [5] recently showed that sub-Angstroem lateral resolution and nanometer vertical resolution can be used to localize individual dopant atoms in semiconductor devices. Here, we show how a combination of this technique with image simulations can be used to determine the three-dimensional shape of crystals with atom-by-atom accuracy.

EXPERIMENTAL

In this study we used commercially available TEM specimens consisting of small gold islands on a perforated carbon film, with areas of graphitized carbon [6]. Series of 41 simultaneous annular dark-field (ADF) and bright-field (BF) images were recorded with an aberration-corrected VG Microscopes HB603U dedicated STEM at varying defocuses with 1 nm increment. Intensities in the recorded ADF images are roughly proportional to the square of the atomic number of the scattering atom species, resulting in an atomic number (Z) contrast. STEM can also provide a phase contrast BF image through the use of a small axial collector aperture (equivalent through reciprocity to the condenser aperture of a conventional transmission electron microscope). The lateral resolution was evaluated to be 0.08 nm, resulting in a depth of focus of about 4 nm when using a 23 mrad illumination semi-angle.

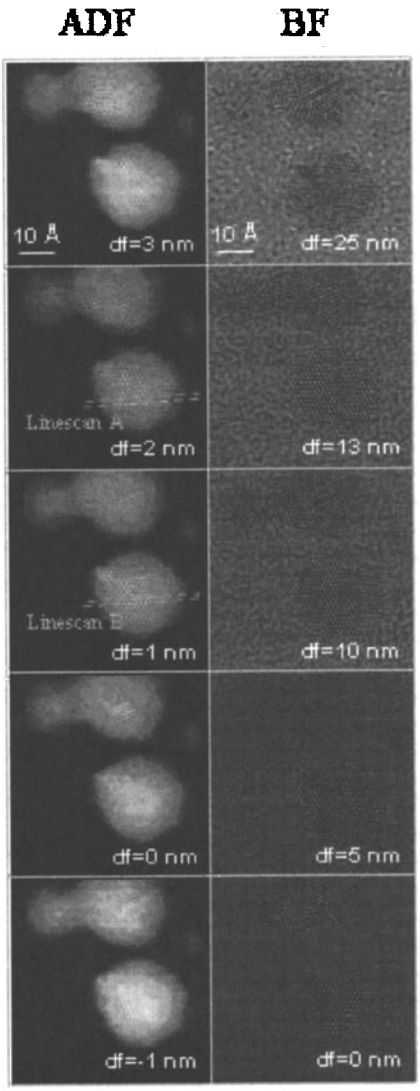

Figure 1: ADF and BF micrographs extracted from a through-focal series. Defocus values dF are calibrated with respect to the Gaussian focal plane.

For the image acquisition, gold particles were chosen which showed a low indexed zone-axis parallel to the optical axis of the microscope. Electron beam currents of the order of 20 pA were used. Each frame of the recorded image stacks was acquired within 8s. After the acquisition, one further frame was recorded to verify that no beam damage occurred. Spatial drift was less than 1 pm/s.

RESULTS AND DISCUSSION

Figure 1 shows five ADF and BF images extracted from one through-focal series. Defocus values relative to the Gaussian focal plane are shown for each frame. The micrographs exhibit 4 gold clusters of which the lower one is found to be in [111] zone-axis orientation with respect to the electron beam. The Au clusters sit on an amorphous carbon support film that is clearly visible in the bright field images but not observable in Z-contrast because of the large contrast differences and the black level settings for the photomultiplier. The ADF micrographs exhibit single Au atoms coming into focus at certain defocus values (see for instance micrographs in Figure 1 taken at 1 and 2 nm defocus). Each single Au atom is observable in 3-4 consecutive frames, indicating a vertical resolution of about 4 nm [5]. Columns of Au atoms in the clusters remain with bright contrast while atom columns in the phase contrast images undergo some contrast inversion between 0 nm and 5 nm defocus.

By thresholding characteristic intensities of the images, isosurfaces were determined from the three-dimensional data set and then used for a three-dimensional reconstruction. In Figure 2, a snapshot of the three-dimensionally reconstructed data set is shown. The single gold atoms are distributed on the carbon matrix around the two large gold

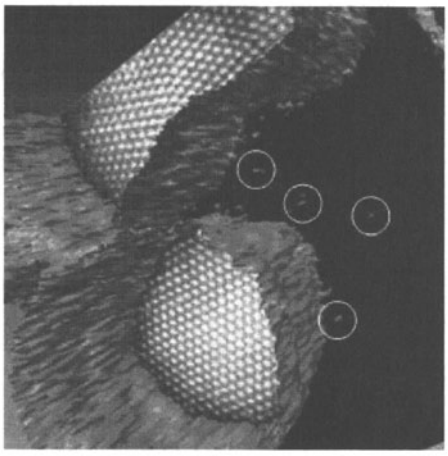

Figure 2: Screenshot of the three-dimensional reconstructed model. The white circles mark single Au atoms present in the vicinity of the Au clusters.

nanoparticles. Some individual Au atoms are visible at different heights throughout the model. In this representation, the top and bottom surfaces of the gold clusters are not resolved because of out-of-focus intensity contributions from the cluster's volume due to the recording in the transmission mode. Therefore, the three-dimensionally shaped Au clusters appear as tubes. In principle, this effect could be removed by an exact knowledge of the three-dimensional probe shape and subsequent deconvolution techniques.

To gather some information about the shape of the Au crystals along the vertical axis, ADF image simulations were performed with imaging parameters determined by the aberration correction software as a function of specimen thickness, i.e. number of Au atoms per column. The simulations show that the optimum defocus for the ADF signal is 2 nm above the first gold atom located in the columns (overfocus). The ADF signal is *linear* with the number of gold atoms for columns containing up to 6 atoms, as it can be inferred from Figure 3. Hence, the number of gold atoms in each column can be determined quantitatively by means of image intensities using this linear relation.

Therefore, we extracted intensity line profiles from across the well-oriented Au cluster (cf. Figure 1) and plotted them in Figure 4. First we extract the signal contributed by a single gold atom at optimum defocus (Figure 2a), namely its maximum intensity out of all the frames. The anomalous background lying between the gold columns could result from the Stobbs factor [7].

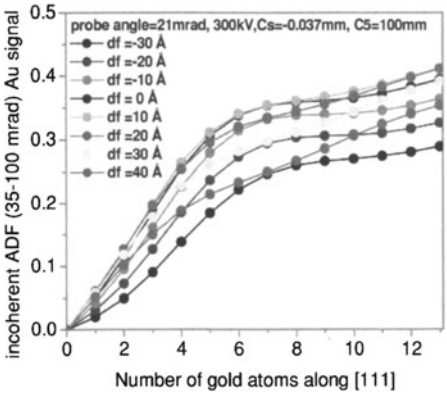

Figure 3: ADF intensity simulations for different defoci as a function of gold atoms per column.

Other possibilities like the chromatic aberration, increased Debye-Waller factors due to low melting points for gold nanoparticles, and the source size broadening effect, have been ruled out by image simulations. Similarly to the technique mentioned above, the maximum signal for any gold column is obtained from Figure 4b.

The number of atoms in each column can thus be estimated with an accuracy of one atom for columns containing up to 5 atoms. For those thicker columns of 20 ~ 40 Å, the error bar is between 2 and 4 atoms.

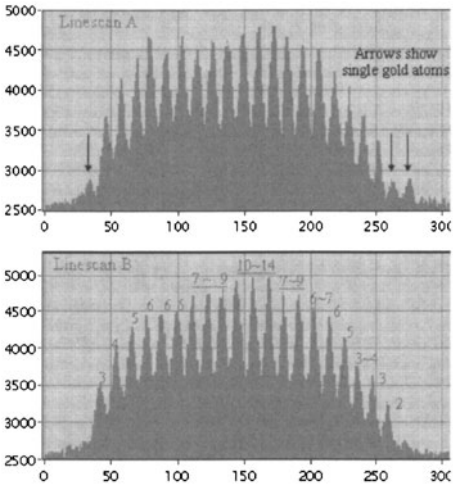

Figure 4: ADF intensity line profiles across one Au cluster as indicated in Figure 1. Black arrows in A depict single atom intensities.

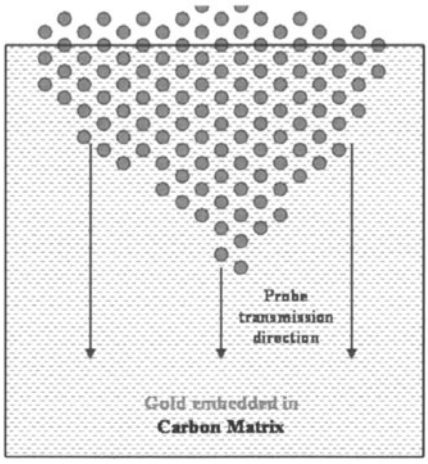

Figure 5: Cross-sectional sketch of the proposed structure model for the investigated Au cluster shown in Figure 1.

The shape of the Au cluster in the vertical direction is depicted using the numbers determined above. The cluster's 3D shape can be also obtained column by column through focal series analysis. Since the best ADF contrast for most columns exists at a defocus of 2 nm above the substrate, one would expect that the top surface of the gold cluster is rather flat and the cluster is mostly embedded in the carbon substrate.

CONCLUSIONS

Aberration-corrected STEM presents a very promising imaging mode via depth slicing. We show that three-dimensional information at near-atomic-scale resolution can be achieved by aberration-corrected STEM combined with image simulation. The main barrier for tomographic imaging is the depth of focus, which can be reduced as the objective aperture becomes larger with future generations of aberration-corrected STEM.

ACKNOWLEDGEMENTS

The authors acknowledge fruitful discussions with A.Y. Borisevich, A.R. Lupini, S.D. Findlay, M.P. Oxley and M.F. Chisholm. This research was sponsored by the Laboratory Directed Research and Development Program of ORNL, managed by UT-Battelle, LLC, for the U.S. Department of Energy under Contract No. DE-AC05-00OR22725 and by an appointment to the ORNL postdoctoral Research Program administered jointly by ORNL and ORISE. K.v.B. is a fellow of the Alexander-von-Humboldt Foundation.

REFERENCES

1 de Rosier, D.J., Klug, A. Reconstruction of Three Dimensional Structures from Electon Micrographs. *Nature* **217**, 130-134 (1968).
2 Midgley, P.A., Weyland, M. 3D electron microscopy in the physical sciences: the development of Z-contrast and EFTEM tomography. *Ultramicroscopy* **96**, 413-431 (2003).
3 Koster, A.J., Ziese, U., Verkleij, A.J., Janssen, A.H., de Jong, K.P. Three-Dimensional Transmission Electron Microscopy: A Novel Imaging and Characterization Technique with Nanometer Scale Resolution for Materials Science. *J. Phys. Chem.* B **104**, 9368-9370 (2000).
4 Miller, M.K., *Atom-Probe Tomography: Analysis at the Atomic level*, Kluwer Academic/Plenum Press, New York (2000).
5 K. van Benthem et al., submitted to Nature (2004)
6 http://www.2spi.com/catalog/standards/othertem7.shtml
7 M.J. Hÿtch, W.M. Stobbs, Ultramicroscopy 53 (1994) 191.

Mater. Res. Soc. Symp. Proc. Vol. 839 © 2005 Materials Research Society

P1.4

Materials analysis by aberration-corrected STEM

Ondrej L. Krivanek, Neil J. Bacon, George C. Corbin, Niklas Dellby, Andrew McManama-Smith, Matthew F. Murfitt, Peter D. Nellist[1] and Zoltan S. Szilagyi

Nion Co., 1102 8th St, Kirkland, WA 98033, USA
[1]Dept. of Physics, Trinity College Dublin, Dublin, Ireland

ABSTRACT

Electron-optical aberration correction has recently progressed from a promising concept to a powerful research tool. 100-120 kV scanning transmission electron microscopes (STEMs) equipped with spherical aberration (C_s) correctors now achieve sub-Å resolution in high-angle annular dark field (HAADF) imaging, and a 300 kV C_s-corrected STEM has reached 0.6 Å HAADF resolution. Moreover, the current available in an atom-sized probe has grown by about 10x, allowing electron energy loss spectroscopy (EELS) to detect single atoms. We summarize the factors that have made this possible, and outline likely future progress.

INTRODUCTION

Adding a Nion spherical aberration (C_s) corrector [1] to a Vacuum Generators (VG) cold field emission (CFEG) scanning transmission electron microscope (STEM) typically improves its resolution by 2-2.5x, to <1 Å at 100 keV and about 0.6 Å at 300 kV. There are now seven aberration-corrected VG STEMs attaining these levels of performance in the field.

The 300 kV aberration-corrected VG HB603 at ORNL, which has now been operating for about 2 years, has been particularly productive, with results such as:

- Direct resolution better than 0.78 Å, unambiguously demonstrated by an HAADF image that resolved the pairs of Si atoms appearing 0.78 Å apart in the <112> projection [2].
- Information transfer to 0.6 Å, shown by the (8,0,4) spacing appearing in the above image.
- Atomic-resolution images of small catalyst clusters and single atoms on alumina [3].
- Elucidation of the detailed atomic structure of an $Al_{72}Ni_{20}Co_8$ quasicrystal, showing that its 10-fold symmetry is broken near the symmetry axis in an energetically favorable way [4].
- Detection of La and Hf dopant atoms in glassy phases at grain boundaries in Si_3N_4 ceramics, at theoretically predicted sites [5].
- Detection of oxygen atoms by HAADF and phase contrast bright-field (BF) STEM imaging of $SrTiO_3$ [6].

A comparable wealth of results has been generated by other C_s-corrected VG microscopes. These include the first-ever demonstration of directly interpretable sub-Å resolution in a single electron micrograph [7], the first identification of a single dopant atom by electron energy loss spectroscopy (EELS) [8], and an unequivocal elucidation of the structure of the $NiSi_2$-Si interface by HAADF imaging [9].

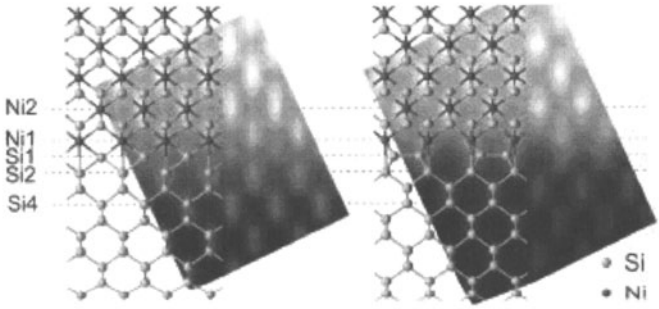

Figure 1. Aberration-corrected HAADF STEM images of the $NiSi_2$-Si interface obtained at 100 kV, with the resultant structure models shown superimposed on the images. The left and right images show the interface viewed in two directions at 90° to each other. Courtesy Drs. U. Falke and A.L. Bleloch, SuperSTEM Laboratory.

The $NiSi_2$-Si interface example (Fig. 1) illustrates the type of problems to which aberration-corrected HAADF STEM imaging can be fruitfully applied. The atomic structure of the interface can be directly read out from the images: the brighter dots correspond to Ni atom columns and the weaker ones to Si columns. At the interface itself, single columns of Si atoms (rather than the dumbbell pair normally present in the <110> projection) can be seen in the left image, and a slight "lean" due to a reconstruction that makes Si atoms at the interface 5-fold coordinated (and thus avoids dangling bonds [10]) can be seen in the right image.

It is interesting to note that the $NiSi_2$-Si interface had been imaged previously, by high resolution phase contrast BF imaging at 400 kV, at about 1.6 Å resolution [11]. The phase contrast images were much harder to interpret, and the derived structure was not in agreement with the one shown here.

The above makes it clear that aberration correction has already made many valuable contributions to materials research, despite being a recent innovation. At the same time, operating aberration-corrected electron microscopes has highlighted various problems, many of them due to the fact that the microscopes that have recently been upgraded with aberration correctors were typically designed 15 to 30 years ago. We are now addressing these problems by developing a completely new microscope, designed for the increased demands of aberration-corrected electron microscopy. Our approach is summarized in the next section.

NEW STEM DESIGN

VG STEMs have many attributes that make them well suited to being upgraded by the addition of an aberration corrector. The chief one among these is the microscope's high-quality cold field emission gun, whose brightness is typically measured to be $>10^9$ A/(cm^2 sr) at 100 kV, i.e. 5-10x brighter than a typical Schottky gun. This gun also delivers an energy spread of 0.3-0.4 eV under standard operating conditions, compared to 0.5-1.0 eV typical of a Schottky gun. This is beneficial for two reasons: it minimizes the resolution loss due to chromatic aberration, and it improves the quality of electron energy loss spectroscopy (EELS) results.